Zurich University
of Applied Sciences

School of
Engineering
ICP Institute of
Computational Physics

Master thesis

Simulating the Electrical Properties of the Human Skin for the Development of Hydration Sensors

Author	Claudio Malnati
Main supervisor	Mathias Bonmarin Daniel Fehr
External supervisor	Gerald Kasting

Date	28.02.2021

Simulating the Electrical Properties of the Human Skin for the Development of Hydration Sensors

Claudio Malnati[a] (Student), Daniel Fehr[a] and Mathias Bonmarin[a]

[a]Zurich University of Applied Science, Institute of Computational Physics, Winterthur, ZH 8401 CH

ARTICLE INFO

Keywords:
skin model
skin hydration
dielectric spectroscopy
stratum corneum

ABSTRACT

A computational model describing the dielectric properties of human skin helps designing, investigating, and optimizing electrodes for dielectric spectroscopy used in skin hydration monitoring. Human skin is composed of several layers with distinct dielectric properties. The hydration state of skin is an important parameter not only affecting the dielectric properties, but also the constitution. The skin model is set up as a multilayer system, each layer resembling its dispersive dielectric behavior with a Cole-Cole model. Focusing on the stratum corneum layer, a hydration model is additionally employed, which simulates the stratum corneum swelling and varies the dielectric parameters under hydration influence. With different fringing-field sensors on top of the multilayer system, the model is numerically evaluated using the finite-element method. Firstly, by means of the stratum corneum hydration model, the range of water concentration was investigated. At normal conditions, i.e. no skin disease, no sweating, no wounds, the water concentration resulted to be higher than 0.585 g/cm^3, or expressed in water activity 0.9745. Secondly, the influence of the hydration dependent stratum corneum thickness on the dielectric spectroscopy was investigated. It was found that the stratum corneum thickness cannot be neglected. In high water concentration range the swelling reduces the capacity, where the capacity would increase, if neglected. Finally, a sensitivity analysis was performed with three different fringing-field electrode types with various geometries. The sensitivity was calculated from the capacity of various hydration levels in relation to the capacity at fully hydrated skin. The analysis confirmed that the electrode sensitivity is influenced by its geometry and dimensions. However, the sensitivity of the impedance electrodes is stronger affected by dimension change than the capacitance electrode.

The models and source code of the project can be found on the ZHAW Github.
https://github.zhaw.ch/malnacla/skinhydration

1. Introduction

Dielectric spectroscopy offers the potential of non-invasive monitoring of skin hydration. Commercially available and well established instruments, such as the MoistureMeterD (Delphin Technology AG), the Corneometer® CM 825 (Courage + Khazaka electronic GmbH), or the Nevisense 3.0 (SciBase AB), are used in dermatology, for analyzing various diseases, and determining the effectiveness of medical therapies [14, 16, 22]. Much work has been invested in optimizing electrodes and developing new technologies. Skin-like or drawn on electrodes have been presented for real time monitoring and wireless measurements [4, 8, 11].

A numerical model resembling the dielectric properties of human skin can help to understand the effects of dielectric spectroscopy within the skin and to study the influence of skin hydration. Various publications characterize biological tissues [6, 20, 21] and report the measurement of dielectric properties of the human skin [2, 15, 19, 28]. A semi-analytic solution for a three layer model of stratum corneum, viable skin, and adipose tissue is proposed [26]. In [10] a model is presented to calculate the effective dielectric properties for each skin layer from numerical cellular structures parametrized by sub-cellular and cellular compounds .

The outermost layer of skin, stratum corneum (SC), functions as a barrier to water loss and as a barrier to exogenous chemical penetration. SC water content is known to reflect skin health and is related to changes in elasticity, flexibility, and surface morphology [3, 7, 25]. Li et al. presented a mass transport model to predict water transport through the SC with a moving boundary for the swelling of the SC. The model of water transport through the SC involves both diffusive and convective transport and can represent both transient hydration and dehydration of the tissue [12, 13].

The objective of this work consists of the development of a reliable, computationally efficient numerical model for the hydration dependent dielectric behavior of the human skin. A multilayer skin model was set up, each layer characterized with its dispersive dielectric properties, in combination with a SC hydration model. Focusing on the SC layer, the dispersive dielectric parameters were fitted to estimate the dielectric properties under hydration influence. To further investigate hydration influences on dielectric spectroscopy, the SC thickness was set up hydration dependent as well.

With the SC hydration model, the range of water concentration was investigated by exposing the skin surface to air at various relative humidities. Three different fringing-field electrodes were employed on the skin model in order to investigate the influence of the hydration dependent SC thickness on the dielectric spectroscopy. Finally, a sensitivity analysis was performed with the three different fringing-field electrode types with various geometries.

ORCID(s): 0000-0003-0227-9247 (M. Bonmarin)

2. Materials and Methods

Different physical models are combined to resemble the behavior of the human skin under dielectric spectroscopy measurements. Various work investigated the SC's hydration influences. A hydration dependency of the dielectric properties is reported in [18], the SC hydration and swelling was investigated in [3], and a swelling model of the SC is proposed in [13]. Therefore, in the final skin model, the SC layer employs a hydration dependency for the dielectric parameters and for the thickness. As previous work showed, the deeper skin layers cannot be neglected [2, 9, 26].

2.1. Stratum Corneum Hydration Model

This section introduces the stratum corneum model as proposed by Li et al. [13]. The final skin model consists of the SC model with no water concentration gradient as described in 2.1.2. The dynamic SC model was used to investigate the hydration and dehydration process and to reproduce measurement steps from previous work for data utilized in this project.

2.1.1. Dynamics of Water Transport in SC

The hydration model of the stratum corneum describes on one hand the hydration profile and the water gradient, and on the other hand the change in the thickness (swelling and shrinking) with varying hydration. The convection-diffusion PDE with moving boundary sufficiently describes the swelling model of the SC.

$$\frac{\partial C_w}{\partial t} = -v\frac{\partial C_w}{\partial z} + \frac{\partial}{\partial z}\Big(D\frac{\partial C_w}{\partial z}\Big), \tag{1}$$

with a water flux

$$f = -D\frac{\partial C_w}{\partial z} + vC_w, \tag{2}$$

where C_w is the water concentration in [g/cm^3], v the convective velocity in [g/cm^{2}s], and D is the diffusivity at depth in [cm^2/s].

The convective velocity is caused by the flux at the lower boundary. It can vary with time but is not depth dependent because it is assumed that the water partial molar volume in the SC is equal to the pure water molar volume.

$$v = \frac{f_0}{\rho_w}, \tag{3}$$

where $f_0 = f(z = 0)$ is the flux at lower boundary and $\rho_w = 1.0\,\mathrm{g/cm^3}$ is the water density. The diffusivity depends on C_w as proposed in [12]

$$D = \frac{1}{10^9}\Big(0.4331 - 0.3765\exp\big(-9.6215C_w\big) + 0.00006428\exp\big(12.873C_w\big)\Big). \tag{4}$$

The moving boundary describes the swelling and shrinking of the SC, where its thickness δ changes with time. The rate of change is defined by the difference of the boundary fluxes, again with the assumption that the water partial molar volume in the SC is equal to the pure water molar volume.

$$\frac{\partial \delta}{\partial t} = \frac{f_0 - f_\delta}{\rho_w}, \tag{5}$$

where $f_0 = f(z = 0)$ is the flux at lower boundary and $f_\delta = f(z = \delta)$ the flux at the skin surface.

If the skin is in contact with air, the flux at the upper boundary is dependent on the relative ambient humidity and can be described as follows:

$$f_\delta = k_g\frac{(a_w - RH)p^\circ_{sat}MW}{RT}, \tag{6}$$

where $k_g = 0.318\,\mathrm{cm\,s^{-1}}$ is the mass transfer coefficient [5], a_w the water activity at the skin surface, RH the relative ambient humidity, $p^\circ_{sat} = 4.76\,\mathrm{kPa}$ is the water saturated vapor pressure at skin surface temperature $T = (32 + 273.2)\mathrm{K}$, $MW = 18\,\mathrm{g\,mol^{-1}}$ is water molecular weight, and $R = 8.314\,\frac{\mathrm{m^3Pa}}{\mathrm{K\,mol}}$ is the ideal gas constant.

2.1.2. SC Equilibrium Water Concentration

In the absence of a water activity gradient, the equilibrium water sorption volume V (g water/g dry tissue) can be calculated using the following equation

$$\frac{V}{V_m} = \frac{cka_w}{(1 - ka_w)(1 - ka_w + cka_w)}, \tag{7}$$

with a_w as the water activity, $c = 4.39$, $k = 1/1.01$, and $V_m = 0.0386$ (g water/g dry tissue). The associated water concentration C_w is related to V according to equation (8)

$$C_w = \frac{\rho_w\rho_{mem}V}{\rho_w + \rho_{mem}V}, \tag{8}$$

with $\rho_w = 1.0\,\mathrm{g/cm^3}$ as water density and $\rho_{mem} = 1.3\,\mathrm{g/cm^3}$ as dry tissue density. With the assumption of constant partial molar volume for water, the equilibrium thickness of the SC δ can then be determined as

$$\delta = \frac{\delta_{dry}}{1 - \frac{C_w}{\rho_w}}, \tag{9}$$

where δ_{dry} is the dry tissue thickness in [µm].

2.2. Dielectric Properties of Skin

Biological tissue is a very heterogeneous material and various components influence the dielectric properties, such as concentration of free water, bound water, and molecular compositions. The dielectric dispersion characteristics (or Debye type dispersion) of biological tissues are commonly approximated by a Cole–Cole model [6, 9, 18, 23]. The human skin is employed as a multilayer model, due to separable dispersive dielectric behavior. In this model, the focus was on three layers; the outer most layer, the stratum corneum, the viable skin, which combines living epidermis and dermis, and the hypodermis as subcutaneous fat. Each

skin layer is represented by a complex relative permittivity $\varepsilon_r = \varepsilon' - j\varepsilon''$ characterized by the Cole–Cole model:

$$\varepsilon_r = \varepsilon_\infty + \sum_n \frac{\Delta\varepsilon_n}{1 + (j\omega\tau_n)^{(1-\alpha_n)}} + \frac{\sigma_{DC}}{j\omega\varepsilon_0}, \tag{10}$$

where ε_∞ is the optical permittivity, n the number of dispersions, $\Delta\varepsilon_n$ is the nth permittivity increment, τ_n is the nth relaxation time, α_n is the nth broadening parameter, ω is the angular frequency, σ_{DC} is the static conductivity, and ε_0 is the dielectric permittivity of the vacuum.

The frequency dependent relationship between the conductivity and realtive permittivity is

$$\sigma = j\omega\varepsilon_0\varepsilon_r, \tag{11}$$

where the conductivity σ and the relative permittivity ε_r are complex quantities [23].

2.2.1. SC Dielectric Hydration Dependency

Naito et al. found that bound water has a negligible influence on the dielectric properties of the SC and recommends to simplify the model to

$$\varepsilon_r = \varepsilon_\infty + \frac{\Delta\varepsilon_{free}}{1 + (j\omega\tau_{free})} + \frac{\Delta\varepsilon_{slow}}{1 + (j\omega\tau_{slow})}, \tag{12}$$

where the $free$ parameters are caused by the free water in SC and the $slow$ parameters are assumed to be caused from protein polarization [18]. The optical permittivity directly depends on the permittivity increment of free water

$$\varepsilon_\infty = 3.3 + \frac{2}{73.2}\Delta\varepsilon_{free}. \tag{13}$$

The value 3.3 represents the relative permittivity of dry SC, which is a typical value for dry protein [1], and the value 73.2 is the realtive permittivity of free water [18].

As stated in [18], the dielectric properties of the SC vary with the hydration of the skin. A linear dependency between the free water content of the SC and the permittivity increment of the free water $\Delta\varepsilon_{free}$ was found. Assuming that all dielectric parameters from (12) undergo the same linear dependency, a linear regression fit can be performed for each parameter to formulate their relation. The equation (7) and (8) are used to formulate the relation between the water concentration and the water activity in equation (14), and therefore the relation of the dielectric parameter with the water activity.

$$C_w(a_w) = \frac{V_m c k \rho_{mem} a_w}{1 + (V_m c k \frac{\rho_{mem}}{\rho_w} - 2k + ck)a_w + (k^2 - ck^2)a_w^2}, \tag{14}$$

where C_w is the resulting water concentration in the SC by given water activity a_w. The linear regression fit resulted in a scaling of C_w because the provided measurements only represent the hydrated state of the SC and no samples for dry tissue are given. The samples and fit parameters are listed in table 1. For complete derivation of the fit see section S2 in supplementary information. The interpolation equations take the following form:

Table 1
Cole-Cole parameters from [18] at three hydration levels used to approximate the SC hydration dependency. β lists the calculated scaling value resulting from the linear regression. $\varepsilon_\infty = 3.3 + \frac{2}{73.2}\Delta\varepsilon_{free}$ can be calculated from $\Delta\varepsilon_{free}$.

	$RH = 40\%$	$RH = 60\%$	$RH = 80\%$	β
$\Delta\varepsilon_{free}$	31.5	33.2	35.9	0.0557
τ_1 [ps]	8	10	10	1.551×10^{-14}
$\Delta\varepsilon_{slow}$	156	250	370	0.432
τ_2 [ns]	6	9	17	1.785×10^{-11}

$$\Delta\hat{\varepsilon}_{free} = \beta_{\Delta\varepsilon_{free}} C_w(a_w), \tag{15}$$

$$\hat{\tau}_{free} = \beta_{\tau_{free}} C_w(a_w), \tag{16}$$

$$\Delta\hat{\varepsilon}_{slow} = \beta_{\Delta\varepsilon_{slow}} C_w(a_w), \tag{17}$$

$$\hat{\tau}_{slow} = \beta_{\tau_{slow}} C_w(a_w), \tag{18}$$

where each dielectric parameter has their own scaling parameter β. $\Delta\hat{\varepsilon}_{free}$, $\hat{\tau}_{free}$, $\Delta\hat{\varepsilon}_{slow}$, and $\hat{\tau}_{slow}$ are the interpolated dielectric parameters.

The final estimated relative permittivity for the SC is formulated as follows:

$$\hat{\varepsilon}_r = \hat{\varepsilon}_\infty + \frac{\Delta\hat{\varepsilon}_{free}}{1 + (j\omega\hat{\tau}_{free})} + \frac{\Delta\hat{\varepsilon}_{slow}}{1 + (j\omega\hat{\tau}_{slow})} \tag{19}$$

2.3. Electrode Model

For dielectric spectroscopy, sensors with different electrode geometries and different electrode setups are available (e.g., multiple electrode pairs, one sensing multiple driving, interdigitated fingers). These sensors can be categorized according to their measurement principle as impedance sensor and capacitance sensor. For impedance measurement, the electrodes are in direct contact with the skin, whereas for the capacitance measurements, the sensors have an insulating layer between electrodes and skin [17].

The dimensions of the electrodes and of the skin are much smaller than the smallest wavelength of the applied signal. Therefore, a quasi-static approximation of Maxwell's equations can be applied with $\nabla \times \vec{E} = 0$. The capacity C of the skin can be calculated by solving the current conservation equations.

$$\nabla \cdot \vec{J} = Q \tag{20}$$

$$\vec{J} = \sigma\vec{E} + j\omega\vec{D} + \vec{J}_e \tag{21}$$

$$\vec{E} = -\nabla V \tag{22}$$

Here $\vec{J}$ is the current density, Q the charge density, $\vec{E}$ the electric field, $\vec{D} = \varepsilon_r\varepsilon_0\vec{E}$ the electric displacement field with ε_r and ε_0 as the relative permittivity and the permittivity in vacuum, $\vec{J}_e$ the external current density, V the applied

Table 2
Cole–Cole parameters for epidermis/dermis (E/D) and for the hypodermis (HYP) layer in the skin model. The values refer to blood for E/D and infiltrated fat for HYP from [6]

	E/D	HYP
σ_{DC} [S m^{-1}]	0.7	0.035
ε_∞	4	2.5
$\Delta\varepsilon_1$	56	9
τ_1 [ps]	8.38	79.9
α_1	0.1	0.2
$\Delta\varepsilon_2$	5200	35
τ_2 [ps]	132.6	15.92
α_2	0.1	0.1
$\Delta\varepsilon_3$	-	33000
τ_3 [ps]	-	159
α_3	-	0.05
$\Delta\varepsilon_4$	-	10^7
τ_4 [ps]	-	15.9
α_4	-	0.01

electric potential, σ the electric conductivity of the material, $\omega = 2\pi f$ is the angular velocity.

2.4. Numerical Analysis

For numerical computation of the above listed models, the finite-element method (FEM)-based simulation software COMSOL Multiphysics® (version 5.6) was used.

As explained in 2.2.1 the dielectric parameters for the SC layer are interpolated with equations (15). In [9] the epidermis/dermis layer was approximated by blood and the hypodermis by infiltrated fat. The dielectric parameters for these two layers were taken from [6] as listed in table 2.

For the evaluation of the water concentration in the SC and the reproduction of the measurements in [18], the SC was initialized as fully hydrated and exposed to a relative humidity of 30% until equilibrium was reached. The 30% of relative humidity was chosen to simulate a realistic dry environment. The reached equilibrium then served as initial SC hydration for the simulation of the hydration boundaries and other hydration levels as investigated in section 3.1. Table 3 summarizes the initial conditions and boundary conditions.

3. Results and Discussion

Under the assumption that the model resembles realistic dispersive dielectric skin behavior, various influences on the electrodes measurements were investigated. The skin model is dimensioned (width, height) so that the boundaries of zero charge $\vec{n}\vec{E} = 0$ do not influence more than 1%, where $\vec{n}$ is the normal vector of the boundary.

As mentioned in section 2.3, different types of fringing-field electrodes are available. In this project, three different electrodes have been used: circular impedance electrode, interdigitated impedance electrode, and interdigitated capacitance electrode. The electrode geometries are illustrated in figure 1a and 1b.

3.1. Range of Hydration Measurement

For better insight of the stratum corneum water concentration range under conditions without special influences (i.e. no sweating, no skin disease, no wounds), the boundaries were evaluated by exposing the SC surface to air with a humidity level of 0% and 100%. The simulation resulted in a water concentration of $C_w = 0.585\,\mathrm{g/cm^3}$ at dry air with 0% relative humidity and $C_w = 0.781\,\mathrm{g/cm^3}$ at humid air with 100% relative humidity, as shown in figures 2a and 2b. A linear relation between dielectric relaxation strength and free water content for water concentration above $0.45\,\mathrm{g/cm^3}$ is proposed in [18]. The measurement range according to the simulation is clearly above $0.45\,\mathrm{g/cm^3}$ and within the linear relation. This justifies the linear approximation of the dielectric parameters in 2.2. Also for this reason, the following investigations were performed in the range with high water concentration.

3.2. Influence of Varying Stratum Corneum Thickness on Measurement

With the changing dielectric SC properties depending on the water content, the question arises what influence the SC thickness, also depending on the water content, has on the measurement. The influence of the varying thickness has been investigated per electrode type at measurement frequency of 1 MHz and compared to the results with constant thickness. In figure 4, 5, and 6, the simulated capacity of the three different electrode types is displayed in relation of the water activity a_w.

The figures 4, 5, and 6 indicate that for all electrode types with varying thickness, the capacity first increases with increasing water activity and drops again at water activity $a_w > 0.95$. Further, with constant thickness, the capacity increases with increasing water activity.

The following points must be considered when interpreting the simulated effects of the comparison of skin with SC swelling with skin with constant thickness. The major component of simulated capacity is due to the electric field that penetrates into the epidermis/dermis layer because it has higher relative permitivity than SC, see tables 1 and 2. If the SC is swelling due to hydration, the electric field penetrates less deep into the epidermis/dermis, hence less capacity.

The increase of the capacity for water activity $a_w < 0.95$ and a decrease for $a_w > 0.95$ can be hypothesized due to the non linear swelling of the SC as seen in figure 3. For water activity $a_w < 0.95$, the SC thickness varies less than 5 µm. The SC relative permittivity increases with the water activity as explained in section 2.2.1. Therefore, for water activity $a_w < 0.95$, the increase of the capacity due to increasing relative permittivity is bigger than the reduction of the capacity due to increasing SC thickness. Due to the non-linearity of the SC swelling, the SC thickness increases about 30 µm in water activity $a_w > 0.95$. In that high water activity range, the reduction of the capacity due to SC thickness is stronger than the increase from the SC relative permittivity. Therefore, a decrease in capacity is observed compared to lower water activities.

Table 3
Initial conditions (IC) and boundary conditions (BC) used to evaluate the water concentration in the SC. The inner boundary is connected to the epidermis and is assumed to always be fully hydrated $C_w = 0.781\,\mathrm{g/cm^3}$. The initial conditions for the hydration steps are the resulting equilibrium of the first step to simulate normally hydrated skin. During all steps, the skin is exposed to air. Therefore, the flux f_δ is dependent on the ambient relative humidity according to (6).

Step	IC	BC at $z = 0$	BC at $z = \delta$
(1) Dehydration	$C_w = 0.781\,\mathrm{g/cm^3}$	$C_w = 0.781\,\mathrm{g/cm^3}$	$RH = 0.3,\ f_\delta$
(2) Dehydration	result of step (1)	$C_w = 0.781\,\mathrm{g/cm^3}$	$RH = 0,\ f_\delta$
(3) Hydration	result of step (1)	$C_w = 0.781\,\mathrm{g/cm^3}$	$RH = 0.4,\ f_\delta$
(4) Hydration	result of step (1)	$C_w = 0.781\,\mathrm{g/cm^3}$	$RH = 0.6,\ f_\delta$
(5) Hydration	result of step (1)	$C_w = 0.781\,\mathrm{g/cm^3}$	$RH = 0.8,\ f_\delta$
(6) Hydration	result of step (1)	$C_w = 0.781\,\mathrm{g/cm^3}$	$RH = 1,\ f_\delta$

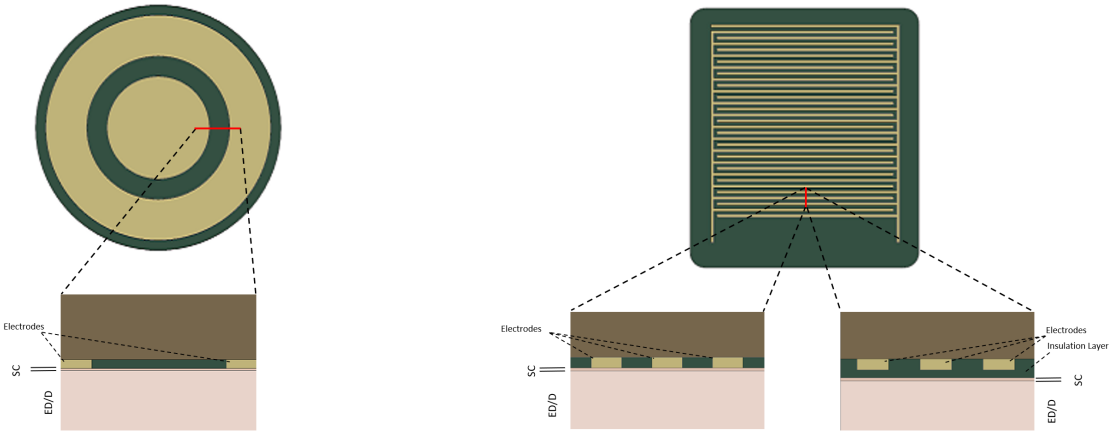

(a) Circular impedance electrode with the outer driving and inner sensing electrode. The zoom illustrates a vertical cut through the electrode and the contact with the skin.

(b) Electrode with interdigitated fingers. The zoom to the left shows a vertical cut through the electrode and the skin contact of the impedance version. The zoom to the right displays a vertical cut through the electrode and the capacitance version with an insulation layer between electrode and skin.

Figure 1: Illustration of the different electrode geometries.

The magnitude difference between the variable and constant thickness is again due to the influence of the epidermis/dermis layer. At constant thickness (here at dry thickness 9.55 µm), the electric field propagates deeper into the epidermis/dermis than with variable thickness and results therefore in higher capacity.

According to this model, varying the thickness depending on the hydration level has a significant impact on the calculated capacity that cannot be neglected. The penetration depth of the electric field could also be investigated by increasing the SC thickness until the capacity converges and the influence of the epidermis becomes negligible.

3.2.1. Influence of Varying Stratum Corneum at Various Frequencies

The figures 7, 8, and 9 show the influence of the varying thickness at logarithmically spaced frequencies from 10 kHz to 1 GHz. It is visible that with increasing frequency the magnitude of the simulated capacity decreases. The trend of the capacity with varying water activity due to SC swelling has an effect throughout all frequencies with a turning point at $a_w \sim 0.95$.

This effect is as expected. The drop in the magnitude of the capacity with increasing frequency can be explained with the SC dielectric spectrum, see S1. In the frequencies of 1 MHz and lower, the SC relative permittivity is dominated by bound water and protein polarization. At frequencies above 1 MHz, the β-dispersion occurs and the relative permittivity is more and more dominated by free water.

3.3. Electrode Dimension Sensitivity

The sensitivity analysis is performed at different SC hydration levels within a water activity range of $a_w = 0.8$ to 0.996 at 1 MHz on the three fringing-field electrode types: circular impedance electrode, interdigitated impedance electrode, and interdigitated capacitance electrode. For each electrode, the relative capacitive sensitivity was calculated with

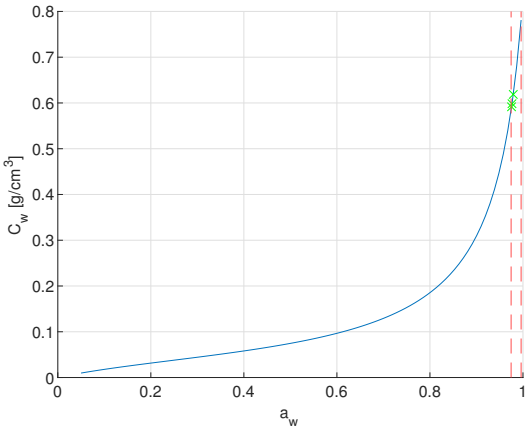

(a) Blue line is the water concentration C_w in relation to the water activity a_w. The red dashed line to the left marks the water activity at ambient relative humidity of 0% at $a_w = 0.9745$ according to equation (7) and (8). The red dashed line to the right marks the water activity at ambient relative humidity of 100% at $a_w = 0.996$, which is equal to fully hydrated SC.

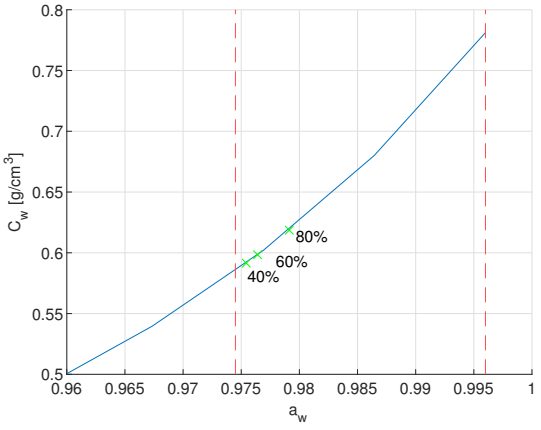

(b) Zoom of the water concentration C_w in relation to the water activity a_w into the marked range. The three green marks on the blue line indicate the resulted water concentration of the SC exposed to ambient relative humidity of 40%, 60%, and 80% for 30 min, see S2.

Figure 2: Water concentration and water activity relationship.

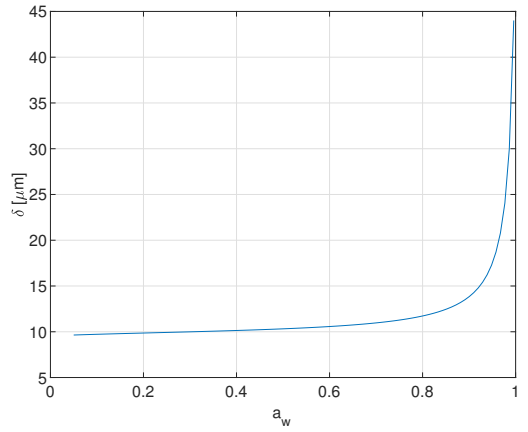

Figure 3: The blue line indicates the SC thickness in relation to the water activity according to equations (7), (8), and (9). The dry SC thickness is 9.55 µm. The non-linearity is clearly visible. In the low water activity range $a_w < 0.95$, the SC thickness only grows approximately 5 µm. However, in the higher water activity range $a_w < 0.95$, the SC thickness grows final approximately 30 µm

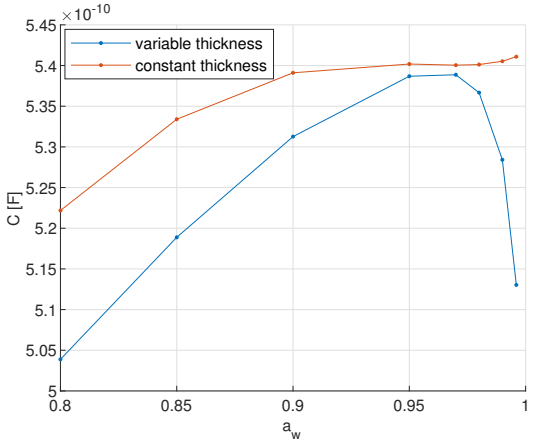

Figure 4: Comparison of the capacity simulation with the circular impedance electrode of the varying thickness in blue and constant thickness in red. The dimensions of the skin are for epidermis/dermis 1 mm and for hypodermis 2 mm. The dry SC thickness in (9), as well as the constant thickness is set to 9.55 µm. The influence of the of the varying thickness is specially visible in the higher water activity range, where the capacity reduces with varying thickness but increases with constant thickness.

the equation (23) in relation to the simulated capacity at fully hydrated level of $a_w = 0.996$. The influence of the electrode dimensions is investigated by varying the electrode's size and the gap between the electrodes. The areas of the driving and sensing electrode are always kept equal.

$$r = \frac{C_{a_w} - C_{0.996}}{C_{0.996}} \tag{23}$$

where C_{a_w} is the simulated capacity in [F] at specified water activity a_w, $C_{0.996}$ is the simulated capacity in [F] at water activity $a_w = 0.996$, and r is the resulting relative sensitivity.

In figure 11a and 11b, it is visible that with reducing both, the electrode gap and the electrode size of the circular impedance electrode, the sensitivity increases. In figure 12a, the sensitivity of the interdigitated impedance electrode reaches an optimum at electrode gap close to 0.12 mm. In figure 12b however, it is visible that the sensitivity increases with increasing the electrode width. The interdigitated capacitance electrode shows two different sensitivity ranges with the border at $a_w \sim 0.95$. Both figure 13a and 13b show increasing sensitivity with increasing electrode gap and width at high water activity of $a_w > 0.95$. At low water activity $a_w < 0.95$ however, the electrodes with wider gap are more

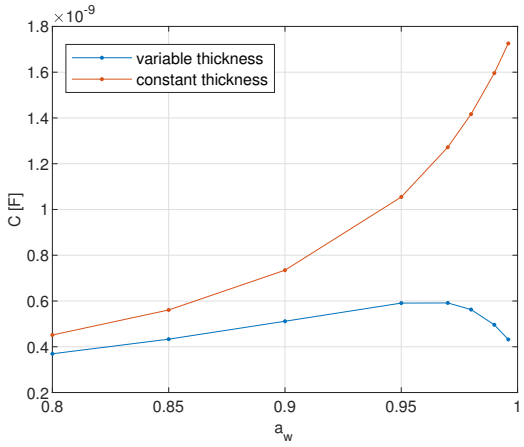

Figure 5: Comparison of the capacity simulation with the interdigitated impedance electrode of the varying thickness in blue and constant thickness in red. The dimensions of the skin are for epidermis/dermis 1 mm and for hypodermis 2 mm. The dry SC thickness in (9), as well as the constant thickness is set to 9.55 µm. The influence of the of the varying thickness is visible over the complete water activity range. The capacity grows exponentially with constant thickness, where the capacity with varying thickness increases linearly with lower water activity and reduces at high water activity.

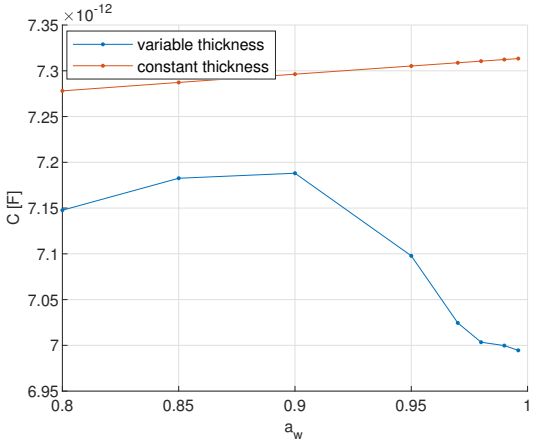

Figure 6: Comparison of the capacity simulation with the interdigitated capacitance electrode of the varying thickness in blue and constant thickness in red. The dimensions of the skin are for epidermis/dermis 1 mm and for hypodermis 2 mm. The dry SC thickness in (9), as well as the constant thickness is set to 9.55 µm. The influence of the of the varying thickness is visible over the complete water activity range. The capacity grows linearly with constant thickness, where the capacity with varying thickness first increases with lower water activity and reduces at high water activity.

sensitive. In contrary, in the same low water activity range, the smaller the electrode width, the more sensitive.

Comparing the values of three electrode's relative sensitivity, in the hydration range $a_w < 0.95$, the sensitivity values of the impedance electrodes are ten times higher than the sensitivity values of the capacitance electrode. In the

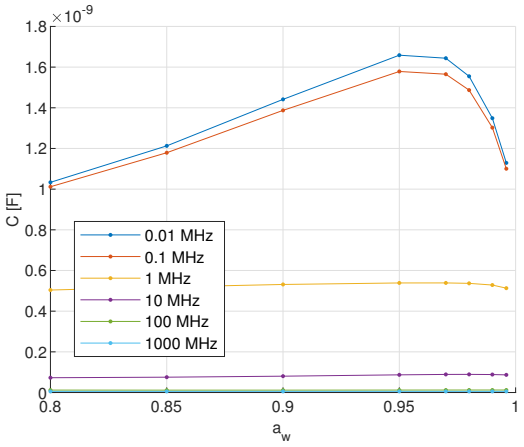

Figure 7: Capacity simulation of the circular impedance electrode at logarithmically spaced frequencies from 10 kHz to 1 GHz. The dimensions of the skin are for epidermis/dermis 1 mm and for hypodermis 2 mm. The dry SC thickness in (9) is set to 9.55 µm. The dispersive dielectric behavior is visible with the capacity reducing with increasing frequency.

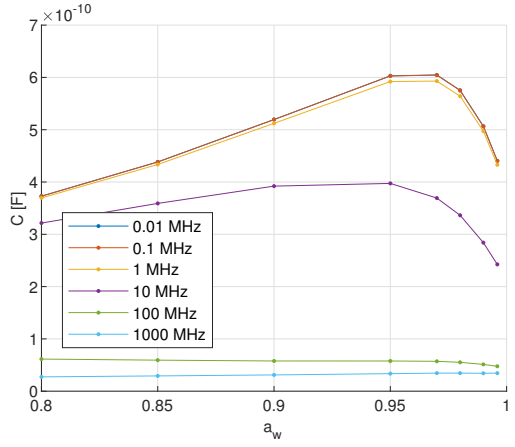

Figure 8: Capacity simulation of the interdigitated impedance electrode at logarithmically spaced frequencies from 10 kHz to 1 GHz. The dimensions of the skin are for epidermis/dermis 1 mm and for hypodermis 2 mm. The dry SC thickness in (9) is set to 9.55 µm The dispersive dielectric behavior is visible with the capacity reducing with increasing frequency.

higher hydration range with $a_w > 0.95$, the sensitivity of the impedance electrodes is even up to a multiple of 100 times higher. Thus, the sensitivity of the impedance electrodes are stronger affected by geometry change than the capacitance electrode.

The current density of the circular impedance electrode in figure 10a indicates that the charge exchange mainly occurs at the edge between the electrodes. Therefore, it is assumed that by reducing the electrode dimensions, the charge density increases and with it the sensitivity. However, this hypothesis is contradictory to what is observed in the sensitivity analysis of the interdigitated impedance electrode, where the sensitivity increases by increasing the dimensions.

An optimum of the electrode becomes visible in figure

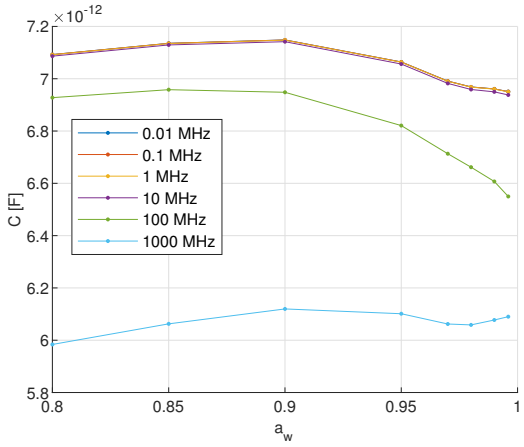

Figure 9: Capacity simulation of the interdigitated capacitance electrode at logarithmically spaced frequencies from 10 kHz to 1 GHz. The dimensions of the skin are for epidermis/dermis 1 mm and for hypodermis 2 mm. The dry SC thickness in (9) is set to 9.55 µm. The dispersive dielectric behavior is visible with the capacity reducing with increasing frequency.

12a. However, for the other geometry sweeps, neither an optimum nor a convergence in the sensitivity is found. The optimum might be out of the examined geometry range or only exists at zero or infinity.

Due to time restriction, these points could not be further investigated in this work.

4. Conclusion

The model reported in this work can represent the human skin for dielectric spectroscopy. Dielectric dispersive parameters are used for each layer of the skin model. The outer most layer, the SC, implements a swelling model and hydration dependency for the dielectric parameters.

Exposing the SC surface to completely dry air with ambient relative humidity of 0% and maximally humid air with ambient relative humidity of 100% brought insight of the water concentration range, and accordingly of the water activity range occurring in the SC. With a water concentration C_w between 0.585 g/cm^3 and 0.781 g/cm^3, or expressed in water activity a_w between 0.9745 and 0.996, the SC is always very hydrated.

Comparing the simulated capacity of the skin model with constant SC thickness to the model that employs the SC swelling, the influence of the varying SC thickness was investigated at various hydration levels. It was found that the more the electric field penetrates into the epidermis/dermis layer, the higher the resulting capacity due to the comparatively high dispersive dielectric parameters of the epidermis/dermis layer. Varying the SC thickness depending on the hydration level influences the penetration depth of the electric field into the lower skin layers. At high water activity of $a_w > 0.95$, the SC thickness reduces the penetration depth into the epidermis/dermis layer and with it the capacity stronger than the SC relative permittivity can compensate for. Hence, a reduction in the total capacity is calculated compared to lower hydration levels. Therefore, the SC swelling has an influence that cannot be neglected in dielectric spectroscopy.

The sensitivity of three different fringing-field electrode types was examined. The analysis showed that the sensitivity is geometry and dimension dependent. Also, the conductive electrodes produce sensitivity values up to a multiple of 100 times higher than the capacitive electrode. Thus, the sensitivity of the impedance electrodes are more strongly affected by dimension change than the capacitance electrode.

4.1. Outlook

This work brings many opportunities and optimization possibilities.

The SC hydration model predicts a non-linear water concentration depth profile. Incorporating this depth dependent water concentration into the SC dispersive dielectric parameter model, the relative permittivity could not only be hydration dependent but also depth dependent.

To improve the dispersive dielectric SC model depending on the hydration, more sample points of dielectric parameters are necessary. With more data, the non-linearity of the hydration dependency could be reproduced. Preferable to a data fit of higher order with more samples, the dielectric properties of the SC can be studied and explained as a physical function depending on the hydration and frequency.

The human skin varies in thickness, functionality, and morphology depending on the anatomical location [24, 27]. The reported model could be used to simulate different skin dimensions by adjusting the thickness of the stratum corneum, epidermis/dermis, and hypodermis, to study specific body location, such as palm, forearm, or forehead. Further, depending on body location, the influence of lower tissue layers may need to be accounted for, such as muscle or bone.

Regarding the electrode geometries, optimization problems could be formulated to solve for the optimal geometries and shape. The design of new electrode geometries can be investigated and analyzed before the production of functional models or prototypes.

5. Acknowledgments

I would like to thank Mathias Bonmarin and Daniel Fehr for the opportunity to participate in this project. I appreciate their support and patience during this thesis and the whole time of my master studies. Fruitful discussions and critical questions kept me on the right track and brought me forward.

I am grateful to my wife Katherine Ankudinov for her love, support, and for editing this report.

References

[1] Muhamed Amin and Jochen Küpper. Variations in proteins dielectric constants.

[2] Ulrik Birgersson, Erik Birgersson, and Stig Ollmar. Estimating electrical properties and the thickness of skin with electrical impedance spectroscopy: Mathematical analysis and measurements. 3.

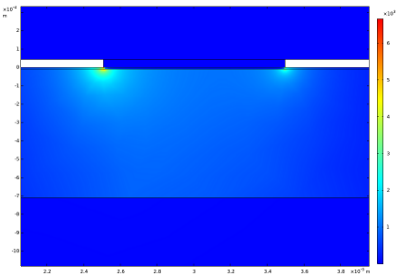

(a) Current density propagation through the skin and inside the circular impedance electrode. The X and Y axis are the size measures of the simulation in [m]. The color gradient, the current density [$\mathrm{A\,m^{-2}}$] shows how the charges penetrate vertically through the SC and move mainly in the epidermis/dermis due to higher conductivity. It is also visible that the charge exchange occurs in the edge between the electrodes and almost no charge leaves the outer surface.

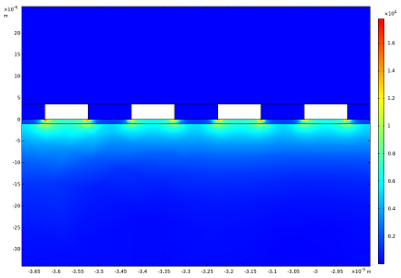

(b) Current density propagation through the skin and inside the interdigitated impedance electrode. The X and Y axis are the size measures of the simulation in [m]. The color gradient, the current density [$\mathrm{A\,m^{-2}}$] shows how the charges penetrate vertically through the SC and move mainly in the epidermis/dermis due to higher conductivity.

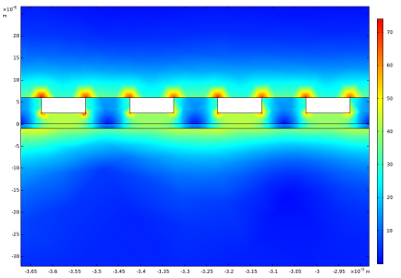

(c) Current density propagation through the skin and inside the interdigitated capacitance electrode. The X and Y axis are the size measures of the simulation in [m]. The color gradient, the current density [$\mathrm{A\,m^{-2}}$] shows that a significant amount of the charges move inside the electrode due to the insulator layer between electrode and skin. The charges that penetrate into the skin again move vertically through the SC and connect in the epidermis/dermis due to higher conductivity.

Figure 10: Illustration of the current density propagation.

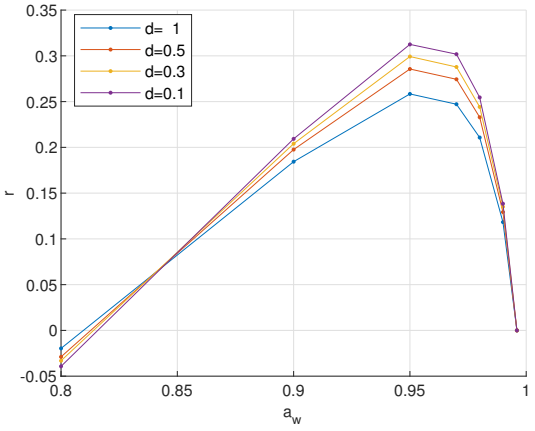

(a) Relative sensitivity r with varying electrode gap of the circular impedance electrode at 1 MHz. d electrode gap in [mm]. The radius of the sensing electrode was kept at 2.5 mm. The radius of the driving electrode was adjusted to keep the area equal to the sensing electrode area. Reducing the electrode gap increases the sensitivity.

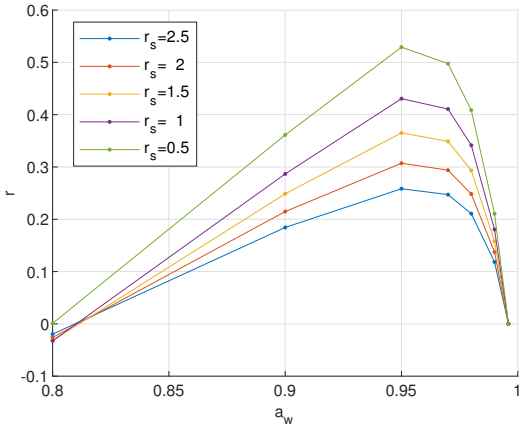

(b) Relative sensitivity r with varying electrode radius of the circular impedance electrode at 1 MHz. r_s is the radius of the sensing electrode [mm]. The electrode gap was kept at 1 mm. The radius of the driving electrode was adjusted to keep the area equal to the sensing electrode area. Reducing the electrode area increases the sensitivity.

Figure 11: Relative sensitivity analysis of the circular impedance electrode.

[3] Agnieszka K. Dabrowska, Christian Adlhart, Fabriziano Spano, Gelu-Marius Rotaru, Siegfried Derler, Lina Zhai, Nicolas D. Spencer, and René M. Rossi. In vivo confirmation of hydration-induced changes in human-skin thickness, roughness and interaction with the environment. 11(3). Accepted: 2018-01-25T10:31:50Z Publisher: American Institute of Physics.

[4] Faheem Ershad, Anish Thukral, Jiping Yue, Phillip Comeaux, Yuntao Lu, Hyunseok Shim, Kyoseung Sim, Nam-In Kim, Zhoulyu Rao, Ross Guevara, Luis Contreras, Fengjiao Pan, Yongcao Zhang, Ying-Shi Guan, Pinyi Yang, Xu Wang, Peng Wang, Xiaoyang Wu, and Cunjiang Yu. Ultra-conformal drawn-on-skin electronics for multifunctional motion artifact-free sensing and point-of-care treatment. 11(1):3823. Number: 1 Publisher: Nature Publishing Group.

[5] H. FREDERICK FRASCH and ANNETTE L. BUNGE. The transient dermal exposure II: Post-exposure absorption and evaporation of volatile compounds. 104(4):1499–1507.

[6] S Gabriel, R W Lau, and C Gabriel. The dielectric properties of biological tissues: III. parametric models for the dielectric spectrum of tissues. page 25.

[7] L.-C. Gerhardt, A. Lenz, N. D. Spencer, T. Münzer,

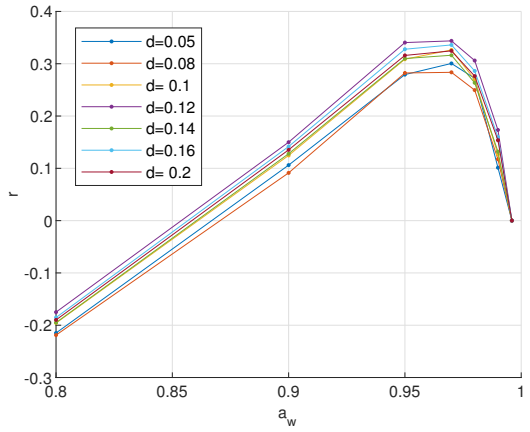

(a) Relative sensitivity r with varying electrode gap of the interdigitated impedance electrode at 1 MHz. d is the electrode gap between the electrode fingers in [mm]. The electrode width was kept at 0.1 mm. An optimum in sensitivity is reached with an electrode gap at $d \sim 0.12$ mm.

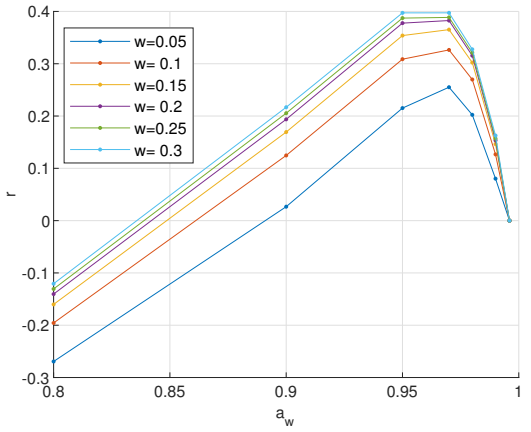

(b) Relative sensitivity r with varying electrode size of the interdigitated impedance electrode at 1 MHz. w is the electrode width of the electrode fingers in [mm]. The electrode gap was kept at 0.1 mm. Increasing the electrode width increases the sensitivity.

Figure 12: Relative sensitivity analysis of the interdigitated impedance electrode.

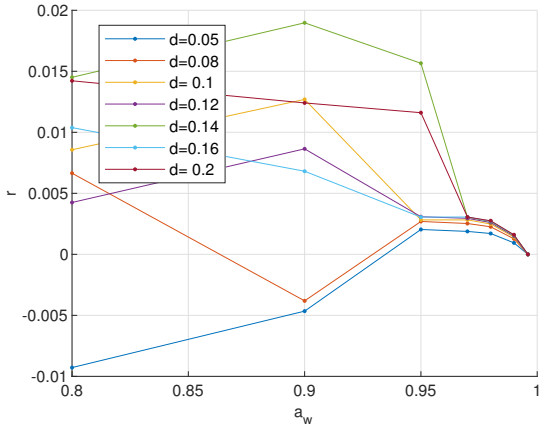

(a) Relative sensitivity r with varying electrode gap of the interdigitated capacitance electrode at 1 MHz. d is the electrode gap between the electrode fingers in [mm]. The electrode width was kept at 0.1 mm. Increasing the electrode gap increases the sensitivity.

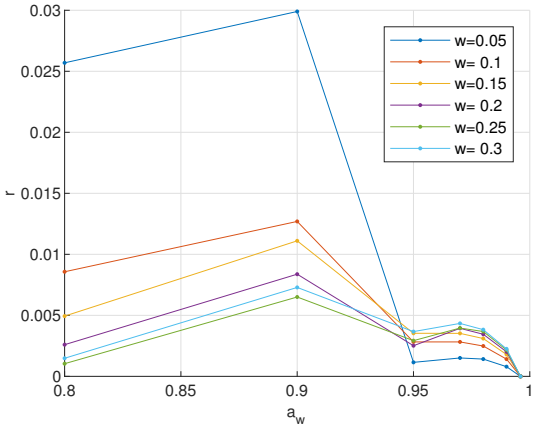

(b) Relative sensitivity r with varying electrode size of the interdigitated capacitance electrode at 1 MHz. w is the electrode width of the electrode fingers in [mm]. The electrode gap was kept at 0.1 mm. In higher water activity range $a_w > 0.95$, the wider the electrode, the better the sensitivity. In lower water activity range $a_w < 0.95$, the smaller the electrode width, the better the sensitivity.

Figure 13: Relative sensitivity analysis of the interdigitated capacitance electrode.

and S. Derler. Skin–textile friction and skin elasticity in young and aged persons. 15(3):288–298. _eprint: https://onlinelibrary.wiley.com/doi/pdf/10.1111/j.1600-0846.2009.00363.x.

[8] Xian Huang, Yuhao Liu, Huanyu Cheng, Woo-Jung Shin, Jonathan A. Fan, Zhuangjian Liu, Ching-Jui Lu, Gil-Woo Kong, Kaile Chen, Dwipayan Patnaik, Sang-Heon Lee, Sami Hage-Ali, Yonggang Huang, and John A. Rogers. Materials and designs for wireless epidermal sensors of hydration and strain. 24(25):3846–3854. _eprint: https://onlinelibrary.wiley.com/doi/pdf/10.1002/adfm.201303886.

[9] Sonja Huclova, Dirk Baumann, Mark Talary, and Jürg Fröhlich. Sensitivity and specificity analysis of fringing-field dielectric spectroscopy applied to a multi-layer system modelling the human skin. 56:7777–93.

[10] Sonja Huclova, Daniel Erni, and Jürg Fröhlich. Modelling and validation of dielectric properties of human skin in the MHz region focusing on skin layer morphology and material composition. 45:025301.

[11] Siddharth Krishnan, Yunzhou Shi, R. Chad Webb, Yinji Ma, Philippe Bastien, Kaitlyn E. Crawford, Ao Wang, Xue Feng, Megan Manco, Jonas Kurniawan, Edward Tir, Yonggang Huang, Guive Balooch, Rafal M. Pielak, and John A. Rogers. Multimodal epidermal devices for hydration monitoring. 3(1):1–11. Number: 1 Publisher: Nature

Publishing Group.

[12] Xin Li, Robert Johnson, and Gerald B. Kasting. On the variation of water diffusion coefficient in stratum corneum with water content. 105(3):1141–1147.

[13] Xin Li, Robert Johnson, Ben Weinstein, Elizabeth Wilder, Ed Smith, and Gerald B. Kasting. Dynamics of water transport and swelling in human stratum corneum. 138:164–172.

[14] Daniele Maggioni, Annamaria Cimicata, Antonella Praticò, Roberta Villa, Ferdinando Bianchi, Silvia Badiale, and Claudio Angelinetta. A preliminary clinical evaluation of a topical product for reducing slight rosacea imperfections. Volume 13:299–308.

[15] Ø G. Martinsen, S. Grimnes, and O. Sveen. Dielectric properties of some keratinised tissues. part 1:stratum corneum and nailin situ.

[16] Harvey Mayrovitz, Daniel Weingrad, and Lidice Lopez. Assessing localized skin-to-fat water in arms of women with breast cancer via tissue dielectric constant measurements in pre- and post-surgery patients. 22.

[17] N. Mazlan, Muhammad Ramli, Mohd Mustafa Al Bakri Abdullah, Dewi Suriyani Che Halin, Siti Salwa Mat Isa, L. Talip, Nuaim Danial, and Sohiful Anuar Zainol Murad. Interdigitated electrodes as impedance and capacitance biosensors: A review. 1885. Journal Abbreviation: AIP Conference Proceedings Publication Title: AIP Conference Proceedings.

[18] Satoru Naito, Masato Hoshi, and Satoru Mashimo. In VivoDielectric analysis of free water content of biomaterials by time domain reflectometry. 251(2):163–172.

[19] Satoru Naito, Masato Hoshi, and Shin Yagihara. Microwave dielectric analysis of human stratum corneum in vivo. 1381(3):293–304.

[20] R. Pethig. Dielectric properties of body tissues. 8(4):5. Publisher: IOP Publishing.

[21] Valerica Raicu, Nobuko Kitagawa, and Akihiko Irimajiri. A quantitative approach to the dielectric properties of the skin. 45(2):L1–L4. Publisher: IOP Publishing.

[22] Esra Saraç, Andreas Meiwes, Thomas Eigentler, Stephan Forchhammer, Lukas Kofler, Hans-Martin Häfner, and Claus Garbe. Diagnostic accuracy of electrical impedance spectroscopy in non-melanoma skin cancer. 100:adv00328.

[23] Sverre Grimnes and Ørjan Grøttem Martinsen. *Bioimpedance and Bioelectricity Basics*. Second edition edition.

[24] H. Tagami. Location-related differences in structure and function of the stratum corneum with special emphasis on those of the facial skin. 30(6):413–434. _eprint: https://onlinelibrary.wiley.com/doi/pdf/10.1111/j.1468-2494.2008.00459.x.

[25] Yuki Tomita, Masashi Akiyama, and Hiroshi Shimizu. Stratum corneum hydration and flexibility are useful parameters to indicate clinical severity of congenital ichthyosis. 14(8):619–624. _eprint: https://onlinelibrary.wiley.com/doi/pdf/10.1111/j.0906-6705.2005.00341.x.

[26] B. Tsai, Erik Birgersson, and Ulrik Birgersson. Mechanistic multilayer model for non-invasive bioimpedance of intact skin. 9:31–38.

[27] Z. Ya-Xian, T. Suetake, and H. Tagami. Number of cell layers of the stratum corneum in normal skin – relationship to the anatomical location on the body, age, sex and physical parameters. 291(10):555–559. Company: Springer Distributor: Springer Institution: Springer Label: Springer Number: 10 Publisher: Springer-Verlag.

[28] Tatsuma Yamamoto and Yoshitake Yamamoto. Electrical properties of the epidermal stratum corneum. 14(2):151–158.